Biosensors and Bioelectronics 26 (2011) 3087–3102

Contents lists available at ScienceDirect

Biosensors and Bioelectronics

journal homepage: www.elsevier.com/locate/bios

Review

Recent progress and continuing challenges in bio-fuel cells. Part I: Enzymatic cells

M.H. Osman, A.A. Shah*, F.C. Walsh

Energy Technology Research Group, School of Engineering Sciences, University of Southampton, University Road, Highfield, Southampton, Hants SO17 1BJ, UK

ARTICLE INFO

Article history:
Received 26 October 2010
Received in revised form
30 November 2010
Accepted 4 January 2011
Available online 6 January 2011

Keywords:
Bio-fuel cells
Enzymatic
Challenges
Immobilization
Materials
Applications

ABSTRACT

Recent developments in bio-fuel cell technology are reviewed. A general introduction to bio-fuel cells, including their operating principles and applications, is provided. New materials and methods for the immobilisation of enzymes and mediators on electrodes, including the use of nanostructured electrodes are considered. Fuel, mediator and enzyme materials (anode and cathode), as well as cell configurations are discussed. A detailed summary of recently developed enzymatic fuel cell systems, including performance measurements, is conveniently provided in tabular form. The current scientific and engineering challenges involved in developing practical bio-fuel cell systems are described, with particular emphasis on a fundamental understanding of the reaction environment, the performance and stability requirements, modularity and scalability. In a companion review (Part II), new developments in microbial fuel cell technologies are reviewed in the context of fuel sources, electron transfer mechanisms, anode materials and enhanced O_2 reduction.

Contents

1. Introduction

Bio-fuel cells have been defined, in the broadest sense, as systems capable of direct chemical to electrical energy conversion via biochemical pathways (Bullen et al., 2006; Katz et al., 2003; Shukla et al., 2004). Direct electrochemical conversion is a desirable feature since it avoids the thermodynamic limitations associated with combustion, in addition to being more environmentally friendly. The conversion is achieved by coupling an oxidation reaction supplying electrons at the anode with a reduction reaction utilizing electrons at the cathode. These two reaction are electronically separated inside the system to force electrons to flow through an external circuit, while ion movement inside the system maintains charge balance and completes the electrical circuit (see Fig. 1 for an example).

Conventional inorganic fuel cells such as the polymer–electrolyte, direct-methanol and solid-oxide systems (Larminie and Dicks, 2003) rely on expensive rare metal catalysts and/or operate on reformed fossil fuels. In bio-fuel cells (BFCs), the chemical reactions are driven by diverse and abundant bio-fuels and biological catalysts. The production/consumption cycle of bio-fuels is considered to be carbon neutral and, in principle, more

---

* Corresponding author. Tel.: +44 23 8059 8520; fax: +44 23 8059 3131.
E-mail address: A.Shah@soton.ac.uk (A.A. Shah).

0956-5663/$ – see front matter © 2011 Published by Elsevier B.V.
doi:10.1016/j.bios.2011.01.004

Nomenclature

Abbreviations

ABTS	2,2′-azinobis (3-ethylbenzothiazoline-6-sulfonate) diammonnium salt
AlcDH	alcohol dehydrogenase
AldDH	aldehyde dehydrogenase
BFC	biofuel cell
BOD	bilirubin oxidase
CDH	cellobiose dehydrogenase
CF	carbon fiber
CoTMPP	cobalt tetramethylphenylporphyrin
DET	direct electron transfer
EFC	enzymatic fuel cell
FAD	flavin adenine dinucleotide
FDH	fructose dehydrogenase
GDH	glucose dehydrogenase
GOx	glucose oxidase
HQS	8-hydroxyquinoline-5-sulfonic acid
KB	Ketjen black
CP	carbon paper
LDH	lactate dehydrogenase
MEA	membrane-electrode assembly
MEC	microbial electrolysis cell
MFC	microbial fuel cell
MP	microperoxidase
MWCNT	multi-walled carbon nanotubes
NAD	nicotinamide adenine dinucleotide
NR	neutral red
OCV	open circuit voltage
PANI	polyaniline
PBS	phosphate buffer solution
PLL	poly-L-lysine
PPy	polypyrrole
PQQ	pyrroloquinoline quinone
PVP	polyvinylpyrrolidone
SCC	short circuit current
SWCNT	single wall carbon nanotube
TBAB	tetrabutylammoniumbromide

Symbols

E^0	formal potential (V)
j	current density (mA cm^{-2})
K_M	Michaelis constant (mol L^{-1} M)
P	power density
R	resistance (Ω)
$[S]$	substrate concentration (M)
E_{cell}	cell voltage (V)
v	enzymatic reaction rate

sustainable than that of conventional fuel cells (Lovley, 2006). Moreover, biocatalysts could offer significant cost advantages over traditional precious-metal catalysts through economies of scale. The neutral pH and low temperature of operation represents further advantages (Bullen et al., 2006; Shukla et al., 2004).

This review considers major developments in enzymatic and microbial fuel cells over the past five years. Earlier developments will be reviewed briefly to provide context. For more detailed reviews of this work, the reader is referred to Bullen et al. (2006); Davis and Higson (2007); Kim et al. (2006). The review is divided into two parts, the present part focussing on enzymatic systems and Part II on microbial systems (Osman et al., 2010). An introduction to biofuel cells is provided in the next section.

2. The operating principles of a bio-fuel cell

Almost all biochemical processes are catalyzed by enzymes. A group of these proteins, oxidoreductases, are responsible for reactions involving electron transfer, and are the most commonly used enzymes. Different subclasses of oxidoreductases are defined based on the type of substrate they act on, as well as the reaction mechanism (e.g. dehydrogenases, oxidases, and peroxidases).

Bio-fuel cells can be classified according to the biocatalyst. Systems using specific isolated enzymes for at least part of their operation are known as enzymatic fuel cells (EFCs), while those utilizing whole organisms containing complete enzyme pathways are know as microbial fuel cells (MFC). A third, intermediate group based on organelles, namely mitochondria, has recently emerged (Arechederra et al., 2009). Several operational differences between these bio-fuel cell types can be identified immediately. Isolated enzymes are substrate specific, while the diverse enzyme contents of whole organisms can be used for a wide range of fuels. Moreover, a complete breakdown of the organic fuel to carbon dioxide and water is usually only possible with several reaction steps (several enzyme catalysts). This is more easily achieved in MFCs, though it also can be achieved in EFCs with an appropriate combination and cascading of specific enzymes (Arechederra and Minteer, 2009).

A short lifetime is an inherent characteristic of enzymes, even in their natural environment (Kim et al., 2006). This drawback is not as severe in MFCs since the organisms are able to regenerate the required enzymes as part of their natural functioning. These living systems are also able to grow and adapt, a common and advantageous phenomenon observed in MFCs (Kim et al., 2007). Fishilevich et al. (2009) recently developed a microbial fuel cell in which GOx was displayed on the surface of yeast in the anode compartment, with glucose as the fuel and methylene blue as a mediator. The use of micro-organism display in this manner opens up the possibility of self-regenerating enzyme systems from the continuous growth and expression of enzymes on organism surfaces (Boder and Wittrup, 1997).

The microorganism used is either a specific isolated species or a mixed culture. It can be applied directly on the electrodes or used in a suspension, or else the system may be inoculated with a mixed culture in a nutrient solution under specific conditions that will allow it to form a biofilm on the electrode. Due to the living nature of organisms, MFC systems have an initial transient operating period of bacterial growth and adaptation to the electron transport mechanism (to and from the electrodes). EFCs, on the other hand, have a faster response time due to the simpler chemical pathways involved.

Ideally, the cell voltage for a BFC is independent of the current drawn. In practice, the reversible cell voltage is not realized even under open-circuit (zero current) conditions due to a number of losses incurred when the cell is operated. The difference between actual cell voltage (V_{cell}) and the theoretical reversible cell voltage for the overall cell reaction (E_{cell}) at a generated current density j (current I divided by the cross-sectional area of the electrodes, A), is termed the overvoltage. As depicted in Fig. 2, there are three major losses that contribute towards the overvoltage (or 'overpotential', η, for a single electrode): activation overpotentials, ohmic losses and mass-transport (concentration) overpotentials (Clauwaert et al., 2008). The cell voltage at zero current (open-circuit voltage, OCV) E_{OCV} can also deviate from E_{cell} as a result of internal currents and fuel crossover. At steady state, and assuming spatially distributed reactants, the cell voltage can be approximated as follows:

$$V_{cell} = E_{cell} - j\sum_{i} \rho_i l_i - \eta_{act} - \eta_{conc} \tag{1}$$

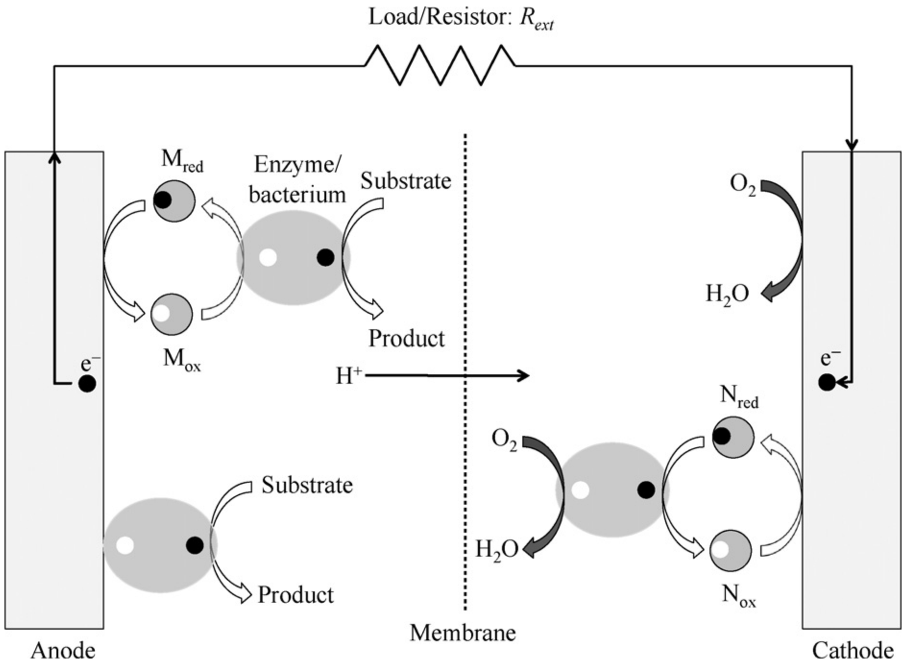

Fig. 1. An example of a biofuel cell with oxygen reduction at the cathode. Oxidation of the substrate is catalysed by the enzymes/bacteria (preferably immobilised on the electrodes), releasing protons and electrons. The electrons released are either transferred directly to the electrode or are transferred via redox mediators, M. Oxygen reduction at the cathode can take place directly on the electrode or via enzymes/bacteria, possibly facilitated by mediators, N. The mediators can be freely suspended or immobilised on the electrode to enhance electron transfer.

where the second term on the right-hand side represents ohmic losses and the final two terms denote the activation and concentration overpotentials, respectively (sums of the contributions from the two electrodes). The reversible potential E_{cell} can be calculated from the Gibbs free energy change for the anodic and cathodic reactions.

At low currents, activation (charge transfer) losses dominate; they arise from the energy barrier to charge transfer, from the mediator or bacteria/enzyme to the electrodes. These overpotentials (separate for the two electrodes) can be approximated if expressions for the reaction rates are known, e.g. a Tafel's or Bultler–Volmer's relation. Activation losses can be reduced by improving the electrode catalysis, increasing the electrode surface area, and by optimising the operating conditions (e.g. temperature and pH).

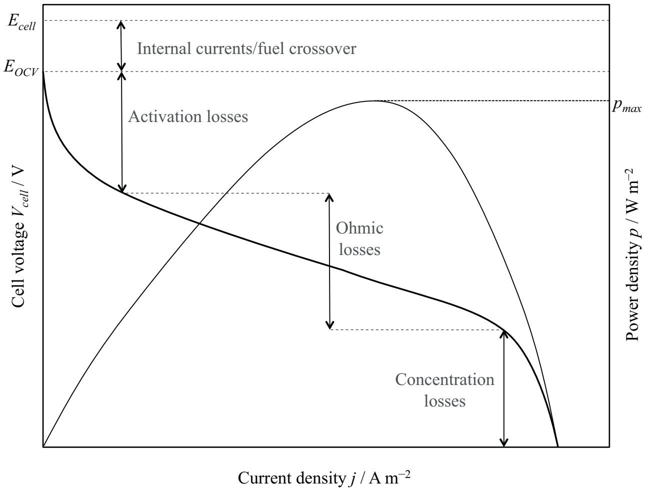

Fig. 2. Typical variations of the cell voltage and power of an operating fuel cell with current density. The major losses of cell voltage and the approximate ranges of current density in which they occur are indicated.

Ohmic losses are due to the resistance to charge transport through the various components in the cell, including contact resistances. They include both ionic and electronic resistances through the current collectors, electrolytes, membrane and electrodes, as well as the interfaces between these components. Assigning a characteristic resistivity ρ_i and thickness l_i to each component i, the ohmic losses may be approximated using Ohm's law, as in Eq. (1). To keep ohmic losses to a minimum, the membrane must possess a low resistance, the gap between the electrodes should be optimal and the components must be well contacted. The solution conductivity can also be increased by varying its composition, but this must not affect the functioning of the bacteria/enzymes.

Concentration losses are caused by resistance to mass transport, leading to large concentration gradients, notably in the vicinity of the electrode surface. These losses tend to dominate at high current densities. They can be lowered by ensuring that the solutions are well-mixed (e.g. by stirring or recirculation) or, in the case of an air-breathing cathode, that the ingress of O_2 is not severely restricted. The electrical power density, P of a BFC is defined as the product of the cell voltage and the generated current density: $P = IV_{cell} = V_{cell}^2/R_{ext}$, where R_{ext} is a known, fixed external resistance. The power density can be calculated by normalising the power with respect to the electrode cross-sectional area or the electrode volume. A typical profile for the power density, $p = P/A = jV_{cell}$, as a function of current density is shown in Fig. 2.

One of the most important measures of performance of a BFC is the coulombic efficiency, which is defined as ratio of coulombs transferred from the substrate to the anode, to the theoretical maximum coulombs produced if all of the substrate is oxidized ($\times$100%) (Liu et al., 2005a). The major causes of reduced coulombic efficiency are (a) the occurrence of alternative reactions that do not result in current production; (b) build-up of biomass; and (c) crossover of the substrate or mixing of the anodic and cathodic reagents, a particular problem in membrane-less systems (Clauwaert et al., 2008).

The operating voltage of a fuel cell has an upper limit dictated by the difference in potential between the oxidant and reductant

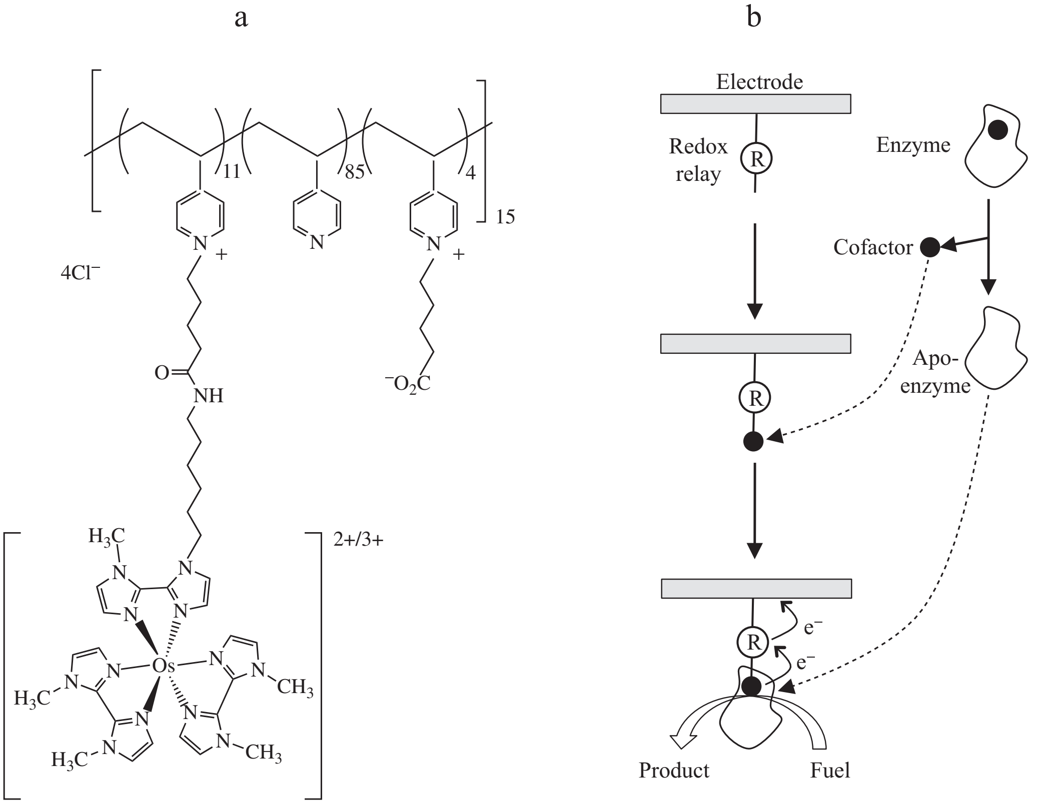

Fig. 3. The structure of polyvinylpyridine-[Os(N,N′-dialkylated-2, 2′-biimidazole)$_3$]$^{2+/3+}$ (Mao et al., 2003). A tris-dialkylated *N*, *N*′-biimidazole Os$^{2+/3+}$ complex was tethered to the backbone of a PVP polymer via 13-atom spacers. (b) Illustration of the concept of enzyme reconstitution. An electron relay unit (molecule, redox polymer or nanoparticle) is linked to an electrode. The cofactor of the enzyme is eliminated and tethered to the relay unit. The apoenzyme is then reconstituted on the relay-cofactor monolayer. Adapted from Zayats et al. (2008).

and the potential difference between the final electron donor and initial acceptor at the electrodes. In bio-fuel cells, this upper limit is determined largely by the redox potential of the active sites acting on the substrate. If mediators (redox active species) are used to shuttle the electrons to/from the electrode, inevitable thermodynamic losses will occur; the mediators require a potential that is shifted from that of the active site to promote electron transfer. Mediated electron transfer can, however, yield higher currents when the mediator concentration is sufficiently large (Kamitaka et al., 2007).

Many reports have categorized BFCs into direct and mediated electron transfer (DET and MET respectively), with often differing definitions. Systems utilizing non-diffusive mediators that are attached along with enzymes on electrodes, or those utilizing mixtures of carbon nanotubes and redox polymers, for instance, can be considered both direct and mediated. Other reports have classified systems based on the materials and methods used for electrode preparation, such as apoenzyme reconstruction, immobilization in redox polymers and the use of nanostructured elements (Kim et al., 2006; Willner et al., 2009; Sarma et al., 2009). In this review, discussion will be divided according to the methods and purposes.

MET usually refers to cases where a mediator is used to enhance electron transfer between the electrochemically active part of the enzyme and the electrode. Conversely, the transfer of electrons directly from the enzyme to the electrode is termed as DET. The vast majority of enzymes are not capable of DET (Sucheta et al., 1993; Ghindilis et al., 1997; Ferapontova et al., 2003; Tasca et al., 2008a) so that most systems employ a mediator, which is usually enzyme specific. For glucose oxidation on glucose oxidase (GOx), examples of mediators are ferrocene monocarboxylic acid, pyrroloquinoline quinone (PQQ), methylene blue, ferrocenecarboxaldehyde and ferrocenemethanol (Harper and Anderson, 2010). The potential applications of bio-fuel cells are diverse. Non-electrochemical applications of bacterial reactions for the production of hydrogen through fermentation, or methane via methanogens are known technologies. Although these bioreactors may be connected to conventional fuel cells for electricity production, either as an external unit supplying the fuel (Ishikawa et al., 2006), or by incorporating the fuel production process with the oxidation reaction on the same anode (Niessen et al., 2005), the biological pathway remains separate from the process of electricity production.

3. Secondary fuel production

Microbial electrolysis cells (MECs) are similar in configuration to microbial fuel cells but require an electrical energy input to initiate a normally unfavorable reaction producing a secondary fuel. For example, hydrogen can be produced on an anaerobic cathode by the reduction of protons (the product of acetic acid oxidation at the anode) (Liu et al., 2005b; Rozendal et al., 2006; Call and Logan, 2008). The electrode reactions can be written as (Liu et al., 2005b):

$$\text{Anode}: \mathrm{CH_3COOH} + 2\mathrm{H_2O} \rightarrow 2\mathrm{CO_2} + 8\mathrm{e}^- + 8\mathrm{H}^+ \quad (2)$$

$$\text{Cathode}: 8\mathrm{H}^+ + 8\mathrm{e}^- \rightarrow 4\mathrm{H_2} \quad (3)$$

which can be combined with the fermentation of glucose into acetate to produce hydrogen.

In another example Cheng et al. (2009) produced methane at a cathode by 'electromethanogenesis' combined with the oxidation of an organic fuel at the anode. Several reports have suggested a mechanism of methane production in microbial electrochemical cells from acetate through acetoclastic methanogenesis, or from the intermediate hydrogen product. The work of Cheng et al. (2009) presents preliminary evidence that methane can be produced from microorganisms (combined with CO_2 capture). MECs that use electricity for the production of a secondary fuel may be used with renewable energy systems to generate usable fuels that are easily transported and stored. Call and Logan (2008) have projected that such systems can provide hydrogen gas at $0.62 per kg compared to $3.8 per kg by water electrolysis. Another class of microbial electrochemical cells not strictly adhering to the definition of a fuel cell is that based on phototroph organisms that use light energy to produce electricity. A two-step approach where *Rhodobacter sphaeroides* converts sunlight and an organic substrate into hydrogen gas, which is then oxidized at a Pt anode, has achieved power densities up to 0.079 mW cm^{-2} (Cho et al., 2008; Rosenbaum et al., 2005) in a single compartment cell. In an approach relying solely on light energy, Furukawa et al. (2006) designed a miniature fuel cell that replicated the photosynthetic/metabolic processes to provide direct electrical energy in light/dark conditions, via alternate conversion between CO_2, H_2O and electricity. Cao et al. (2008) used an enriched consortium of phototrophic bacteria from a wastewater treatment plant in a two-chamber MFC. A maximum power density of 0.265 mW cm^{-2} was obtained. A sediment type MFC using mixed communities of photosynthetic and heterotrophic microorganisms, capable of power production in both light and dark without the need of organic substrate additions, was recently reported by He et al. (2009).

4. Applications of bio-fuel cells

An immediately obvious area of application is static power generation, with microbial fuel cells being the more likely candidate. These systems can be fuelled by widely available, carbon-neutral complex fuels such as cellulose (Ishii et al., 2008; Niessen et al., 2005). Alternatively, they can form the basis for waste treatment systems, combined with energy generation from the organic matter found in sewage. In this application area, MFCs will have to compete with traditional anaerobic digesters producing methane or hydrogen. At present, this is not possible considering target power densities of around 1 kW m^{-3} for economic competitiveness (Watanabe, 2008; Rabaey and Verstraete, 2005). Despite these drawbacks, direct electrical output with high efficiency, low operating temperatures, and good organic treatment efficiency, with the possibility of operating on low strength wastewater, are some of the advantages of MFCs (Watanabe, 2008; Rabaey and Verstraete, 2005). Moreover, bio-electrodes can be used for the oxidation/reduction of specific target substrates (such as nitrate, iron and sulfate) in waste removal or metal extraction from minerals (He and Angenent, 2006). The operation of MFCs on marine sediment to power remote marine instruments has also been explored in several reports.

For applications on a smaller scale, BFCs operating on high energy density fuels have the potential to power portable electronic devices, though current power densities are still far from the target figures of ~100 mW (Sakai et al., 2009). *In vivo* application of bio-fuel cells, either for powering small implantable devices or as biosensors, are more promising for the short term due to their low power requirements. Short life times are, however, a major issue.

5. Biofuel cell designs and configurations

The classical design of an BFC is based on two chambers containing the anode and cathode, separated by a ion-selective membrane (Bullen et al., 2006). Such cells can be operated in either batch or continuous mode. For wastewater treatment (MFCs), an up-flow, two-chamber design was developed by He et al. (2005), operating in continuous mode. The system exhibited a high internal resistance of 84 Ω. A membrane-less version was constructed by Jang et al. (2004), with, however, a considerably higher internal resistance of 3.9 MΩ. Removing the membrane can lead to higher power outputs but the cells must be carefully designed for high reaction selectivity in order to avoid low coulombic efficiencies (due to transport of oxygen to the anode). For scale up and reduced cost, on the other hand, the concept of a membrane-less, single chamber design is highly attractive. Moreover, the use of a ferricyanide solution and aeration in the cathode compartment are not desirable. Park and Zeikus (2003) developed an MFC with a Mn^{4+} graphite anode and air cathode containing an internal, proton-permeable porcelain layer. Liu and Logan (2004) simplified the design by using a carbon-paper air-breathing-cathode (direct O_2 reduction, catalysed by platinum) without a membrane in a tubular arrangement. The cell exhibited a higher power density than an equivalent membrane-containing cell but with a much reduced coulombic efficiency. An alternative arrangement was developed by Rabaey and Verstraete (2005), in which a granular graphite matrix anode was housed in a tubular, sealed membrane covered by a woven-graphite cathode (soaked in a ferricyanide solution).

Immobilisation of the enzymes/mediators opens up the possibility of single compartment EFCs. There are, however, very few examples of membrane-less or separator-free EFCs. The first single-chamber EFC was developed by Katz et al. (1999b), consisting of two immiscible electrolytes separated by a liquid–liquid interface, allowing DET to take place. GOx apo-enzyme was reconstituted a PQQ-flavin adenine dinucleotide phosphate (FAD) monolayer associated with an Au electrode (see Section 7). The cathode consisted of an Au electrode onto which a microperoxidase-11 monolayer was assembled and for which cumene peroxide was used as the oxidiser. Ramanavicius et al. (2005) constructed a single-chamber EFC operating with immobilised alcohol dehydrogenase (AlcDH) on a carbon-rod anode and co-immobilized GOx/microperoxidase on a carbon-rod cathode. The power density, around 10 nW cm^{-2}, was low and the operational half-life was only 2.5 days. A DET, single-chamber H_2/O_2 cell with hydrogenase at the anode and fungal laccase at the cathode was constructed by Vincent et al. (2005), again, however, with a low power density. A more systematic selection of the enzymes and electrode materials by Kamitaka et al. (2007) led to a single-chamber, membrane-less fructose/O_2 cell capable of power densities on the order of 1 mW cm^{-2}; fructose dehydrogenase (FDH) was immobilised on a Ketjen–Black (KB) modified carbon paper and multi-copper oxidases were immobilised on a carbon paper cathode modified with KB and a carbon aerogel. Coman et al. (2008) instead used cellobiose dehydrogenase (CDH) and lacasse for a glucose/O_2 system, which was capable of only 5 μW cm^{-2}. More recently, Wang et al. (2009) immobilised GOx (anode) and laccase (cathode) on porous silicon substrates with pre-deposited carbon nanotubes to form a membrane-less, mediator-free glucose EFC. Again, the power density (1.38 μW cm^{-2}) was low and decreased by a factor of almost 5 after 24 h.

6. Enzymatic fuel cells

The two major problems in enzyme-based systems are the short lifetime of the enzyme caused by a reduction in its stability when functioning in a foreign environment, and the low power densities resulting from a low electron transfer rate from the enzyme active site to the electrode (Kim et al., 2006). The bulk of the research in enzymatic fuel cells has been directed at enzyme/electrode integration methods that alleviate these problems. The short lifetime (a few hours) is an inherent characteristic of enzymes even in their natural environment, but the lifetime may be increased to a few days by immobilization (Kim et al., 2006).

Enzymes used in fuel cells are of the oxidoreductase family (capable of catalysing oxidation and reduction reactions). They can be categorised into three groups, according to the type of electrical communication (Heller, 1992) or to their associated redox cofactors. The first group consists of PQQ-dependent dehydrogenases, e.g. AlcDH, glucose dehydrogenase and glycerol dehydrogenase. Each is structurally different, but most have multiple metal centers and the coenzyme PQQ is bound to the enzyme. The second group includes those with a nicotinamide adenine dinucleotide ($NADH/NAD^+$) or nicotinamide adenine dinucleotide phosphate ($NADPH/NADP^+$) cofactor, e.g. glucose dehydrogenase and AlcDH. In this case, the redox center is usually loosely bound and may diffuse away. This allows the enzyme to transfer electrons to the electrode by the diffusing center, although the diffusing enzyme site may be lost, especially in continuous flow systems. Covalent linking of such enzymes needs to maintain a flexible link, allowing reversible movement between the protein structure and the electron acceptor. Enzymes in the third category have a tightly bound FAD redox cofactor that is buried deep inside the protein structure, which makes extraction of the electrons difficult. The most commonly used enzyme, GOx, belongs to this group. In an aqueous solution, the redox potential of FAD at the enzyme active site is negative, making it ideal for the anode side of a biofuel cell if DET can be achieved. However, systems employing GOx are typically mediated, although it is possible to achieve DET using nanostructured electrodes as discussed later (Xiao et al., 2003; Zayats et al., 2005; Cai and Chen, 2004; Patolsky et al., 2004).

For biological cathodes, the enzymes are typically multi-copper oxidases, which are capable of a four-electron reduction of O_2 to water and have a high specificity towards this reaction (Solomon et al., 1996). Examples include plant and fungal laccases (Chen et al., 2001) and BOD (Mano et al., 2003). Laccases are generally employed under slightly acidic conditions, while BOD has activity in more alkaline media, which allows it to be used at neutral pH. Cytochrome oxidase and cytochrome *c* have also been employed. In the case of H_2O_2 reduction, microperoxidase (Willner et al., 1998a; Katz et al., 1999b) and horseradish peroxidase (Pizzariello et al., 2002) are commonly used as enzymes.

7. Enzyme and mediator immobilization

Immobilisation of the enzyme can has several advantages, including isolation of the enzyme for reaction, increased selectivity, improved mass transfer and long-term stability (Cao, 2005). It also has the advantage of separating the enzyme from the mixture containing the substrate, allowing for more modular cell designs. On the other hand, it can affect the stability and/or activity of the enzyme, it can introduce additional mass-transfer limitations on the substrate and it involves additional costs. Stability is clearly a key consideration. The stability of the immobilised enzyme will depend on the nature and strength of the bonds to the support material, the conditions required for immobilisation, the degree of confinement and the conditions under which the enzyme reactions occur in a functioning electrode. The method of immobilization must be selected carefully to avoid denaturing of the enzymes and loss of structural freedom required for their activity (Moehlenbrock and Minteer, 2008; Cooney et al., 2008).

The main immobilisation techniques for biosensors and EFCs are (Tischer and Wedekind, 2000): physical surface adsorption with diffusional mediators, or mediators co-adsorbed with an enzyme; entrapment in conducting polymer matrices or gels; wiring or covalent attachment to functionalised polymers; and apoenzyme reconstruction. Nano-structured elements can also be used as substrates for binding, or incorporated with one of the aforementioned techniques for enhanced electrical conductivity and stability.

The simplest method of enzyme immobilization is physical adsorption or entrapment. Enzymes can be adsorbed, for example, onto conductive particles such as carbon black or graphite powder (Pizzariello et al., 2002). The methods are straightforward and cost-effective. If the binding forces (primarily electrostatic) between the enzyme and the support are too weak, however, the enzymes can desorb and contaminate the solution; if they are too strong, denaturation can occur during the immobilisation process. Entrapment involves the confinement of the enzyme within a polymer matrix, a sol–gel (Kandimalla et al., 2006), a redox hydrogel (Gregg and Heller, 1991) or behind a semi-permeable membrane. The structure must permit a sufficient degree of enzyme movement, while simultaneously preventing any leaching of the enzyme and/or mediator.

Isolated enzymes can be covalently bonded to supports (e.g. porous glass, cellulose, ceramics, and metallic oxides) via different functional groups on the support and enzyme, often in the presence of enzyme inhibitors. Reagents are used to activate the functional groups on the support. The functional groups on the enzyme, which include amino, carboxylic acid and hydroxyl groups, should not be essential for catalytic activity. The conditions for this type of immobilization are important since they determine the level of enzyme activity retention. Cross-linking consists of joining enzymes to form three dimensional aggregates via covalent bonding between active groups within the enzymes. The aggregates exhibit low mechanical stability and the retained enzymatic activity can be low using this method (Sheldon, 2007).

Covalent bonding and cross-linking are commonly used to immobilise enzymes on self-assembled monolayers (SAMs) (Gooding and Hibbert, 1999). In the context of biosensors, the most studied SAMs are those formed by alkanethiols chemisorbed from solution onto gold surfaces (Dubois and Nuzzo, 1992). Despite the many advantages of these SAMs (simplicity of preparation, densely packed structures and control over functional groups at the monolayer surface), they are prone to instability (Schoenfisch and Pemberton, 1998; Delamarche et al., 1994; Gooding et al., 2003). To improve stability, several research groups have used covalent modification of carbon surfaces via electrochemically reductive adsorption of aryldiazonium salts (Allongue et al., 1997; Saby et al., 1997; Kariuki and McDermott, 2001; Brooksby and Downward, 2004). The resulting monolayers are highly stable over a wide potential window (Allongue et al., 1997). In recent studies, gold, graphite and glassy-carbon (GC) electrodes were functionalised using aryldiazonium salts bearing carboxylic acid groups (Pellissier et al., 2008; Boland et al., 2009a). Pellissier et al. (2008) grafted a GOx layer on a GC electrode modified using this method, through coupling with peripheral amine groups of the GOx. This enzyme layer was used as an anchoring base onto which a cross-linked enzyme layer was subsequently deposited, before testing the electrode using a GC rod counter electrode. The authors demonstrated that these modified electrodes retained much of their activity after 6 weeks, while control electrodes prepared by depositing the cross-linker and GOx directly onto the GC had lost all activity within only 1 week.

Sol–gel glass is produced by the hydrolysis and polycondensation of organometallic compounds (typically silicon alkoxides) at low temperature (Lin and Brown, 1997). Enzymes can be introduced during the formation of the sol–gel (the ‘sol–gel process’), leaving them entrapped around siloxane polymer chains within an inorganic oxide network. The final matrix structure can be controlled by the pH, the temperature, the choice of solvent and the choice of catalyst, amongst other considerations. The main advantages of this method in the context of biosensor and biofuel applications are: simplicity of preparation; the ability to control

Table 1
Summary of key enzymatic fuel cell developments

Anode	Cathode	Electrolytes/membrane	P_{max} (cw cm^{-2})	V or j at P_{max}	OCV (V)	Remarks	Reference
Mitochondria immob. in modified Nafion on C-electrode	Air-breathing **Pt**-C/membrane assembly	10 mM, 7.45 PBS, 6 M $NaNO_3$, 100 mM **pyruvate**, 1 g L^{-1} ADP	0.0315†, 0.024 (average)	0.1† mA cm^{-2}	–	Air cathode/ membrane assembly	Arechederra et al. (2009)
AlcDH/AldDH/oxalate oxidase in modified Nafion on C-paper	Air-breathing **Pt** –C/membrane assembly	7.15 pH PBS, 6 M $NaNO_3$ 100 mM **glycerol**	1.32	2† mA cm^{-2} (0.66 V†)	–	Air cathode/membrane assemble	Arechederra and Minteer (2009)
GOx /HQS (mediator) in PPy on Carbon rod	**Laccase** /ABTS (mediator) in PPy on porous carbon tube	5 pH PBS, 10 mM **glucose**, N_2 purged, 37 °C, separate O_2 solution circulated inside cathode	0.027	0.25 V	0.41†		Brunel et al. (2007)
CDH adsorbed on graphite	**Laccase** adsorbed on graphite	0.1 M citrate buffer, 4.5 pH, 5 mM **glucose**, air saturated	5 × 10^{-3}	0.5 V	0.73	Membrane/mediator-less. Enzyme desorption causes current/power loss.	Coman et al. (2008)
5 bilayers of AuNPs/**GDH** on three dimensional ordered macroporous, cystamine treated Au electrode	Similar to anode, using **laccase** as catalyst	0.1 M, 6 pH PBS, 5 mM NADH, 30 mM **glucose**	0.178	0.226 V	0.32	SCC = 0.752 mA cm^{-2}	Deng et al. (2008)
Cross-linked clusters of **GOx** and CNTs on CF electrode (0.332 cm^2)	Air breathing **Pt** –C cathode (0.332 cm^2)	Un-buffered, 200 mM **glucose**, 10 mM benzoquinone	0.12	0.1 V	0.33	MEA assembly. Better initial performance but degrades quickly in buffered solutions due to cation interference with proton transport.	Fischback et al. (2006)
GDH on poly(brilliant cresyl blue)/SWCNT/GC rod (3 mm diameter)	Cross-linked **BOD** on SWCNT on same carbon electrode	0.1 M PBS, 7 pH, 10 mM NAD$^+$, 40 mM **glucose**, ambient air	0.054	0.5 V	0.73	Membrane-Less. 5% P loss in first day. 46% loss in one week	Gao et al. (2007)
GOx ‘wired’ through PVP-Os complex with cross-linking on 2 cm long, 7 μm diam. CF	**BOD** ‘wired’ through PAA-PVI-Os complex with cross-linking on similar electrode	20 mM PBS, 7.24 pH, 0.14 M NaCl, 15 mM **glucose**, 37 °C	0.315	0.46† V	–	Membrane-less. Commercial enzyme stock purified before usage. Operating cell for 1 week at 0.52 V lost 6% of power output per day	Gao et al. (2009)
$Au_{70}Pt_{30}$ bi-metallic nanoparticles on inner surface of carbon tube (4.4 cm^2, 1.4 cm diam.)	**BOD** /ABTS in modified Nafion on inner surface of porous carbon tube (6 mm diam.)	7.4 pH, PBS, 0.7 M **glucose**, 37 °C	0.19, 0.09 (10 mM glucose)	0.52 V, 0.4 V (10 mM glucose)	0.89†	Abiotic anode. Concentric design. Membrane-less	Habrioux et al. (2009)
FDH adsorbed on Ketjen’s black (0.282 cm^2)	**Laccase** adsorbed on carbon aerogel particles (0.282 cm^2)	McIlvaine buffer, 5 pH, 200 mM **fructose**, O_2 saturated, 25 °C	0.85 (stirred), 0.39 (unstirred)	0.41 V	0.79	SCC = 2.8 mA cm^{-2} (stirred), 1.1 mA cm^{-2} (unstirred). Power drops to 63% after 12 hours. 4 cells in series operate 1.8 V LED for ~60 days.	Kamitaka et al. (2007)
GOx /HQS immobilized in polypyrrole nanowires (0.15 cm^2)	**BOD** /ABTS in polypyrrole film (0.35 cm^2)	7.4 pH, PBS, 15 mM **glucose**	0.28	0.15 V	0.35	SCC = 2.9 mA cm^{-2} and maximum power density with 200 nm diam. 16 μm length nanowires. Membrane-Less	Kim et al. (2009)

Table 1 (*Continued*)

Anode	Cathode	Electrolytes/membrane	P_{max} (cw cm^{-2})	*V* or *j* at P_{max}	OCV (V)	Remarks	Reference
GOx covalently attached to 3-methylthiophene (3MT) and thiophene-3-acetic acid (T3A) copolymer	**BOD** covalently attached to same copolymer	0.1 M PBS, 7 pH and either 0.1 M **glucose**, 1 mM *N*, *N*, *N′*, *N′*-tetramethyl-p-phenylenediamine, N_2 saturated or 1 mM ABTS, O_2 saturated in either compartment separated by Nafion membrane	0.15	0.35 V	0.61	Anodic current decreased to 50% while cathodic current decreased to 75% the initial values after 1 month	Kuwahara et al. (2009)
Au electrode-cystamine-PQQ-**LDH** monolayer	Au electrode-cystamine-**microperoxidase 11**	Anolyte: 0.1 M tris buffer, 7 pH, 20 mM $CaCl_2$, 20 mM NAD^+, 20 mM **lactate**. Catholyte 0.1 M PBS, 7 pH, 1 mM H_2O_2, ABTS. Nafion separator.	0.142	$0.1^{\dagger}$ V	$0.34^{\dagger}$	LDH immobilization carried in presence of $CaCl_2$ promoter, NAD^+, and lactate found to increase power by 26% compared to immobilization without.	Lee et al. (2009)
Latex draw chemical structure **GOx** /single-stranded DNA-wrapped SWCNT on cystamine dihydrochloride treated Au electrode (0.0314 cm^2)	Similar immobilization for **laccase**	0.1 M PBS, 7 pH, **glucose**, O_2, 25 °C	0.442	0.46 V	$1.5^{\dagger}$	Cell operated for more 5 days with power in excess of 0.43 mW cm^{-2}. DNA-wrapped SWCNT found to increase enzyme loading.	Lee et al. (2010)
Polyethylene glycol diglycidyl ether) **GOx** /SWCNTs in silica gel	**BOD** /SWCNT in silica gel	Anolyte: 4 mM ferrocene methanol, 100 mM **glucose**. Catholyte: 8 mM ABTS, O_2 saturated. Room temperature. Nafion separator.	0.12, 0.086 (ambient air)	0.24 V, 0.21 V (ambient air)	0.48		Lim et al. (2007)
Penicillium pinophilum sourced **GOx** /PVP-Os complex, cross-linked, on 2 cm long, 7 μm diam. CF	**Laccase** /PVP-Os complex, cross-linked on 2 cm long, 7 μm diam. CF	20 mM citrate buffer, 5 pH, 37 °C, 5 mM **glucose**	0.28	0.88 V	–	GOx sourced from *P. pinophilum* allows higher power density at lower fuel concentration than tradition *A. niger* but unstable at neutral pH. 3% power loss per day for first 2 weeks.	Mano (2008)
GDH /NAD^+ in Ketjen's black on GC (0.07 cm^2)	**BOD** in Ketjen's black	PBS, 50 mM **glucose**, O_2 saturated	0.052	0.3 V	0.64	SCC = 0.223 mA cm^{-2}. Membrane/mediator-less	Miyake et al. (2009)
AldDH adsorbed on graphite electrode	**AlcOD/microperoxidase-8** adsorbed on graphite electrode	50 mM sodium acetate, 6 pH, 100 mM KCl, 2 mM **ethanol**	1.5×10^{-3}	–	0.24	Ethanol as substrate for both half-reactions. Power decreases to half initial value after 26 h of operation	Ramanavicius et al. (2008)

4 layers of (CF/ poly-L-lysine/ **GDH** /diaphorase/NADH/vitamin K_3/polyacrylic acid sodium salt) (1 cm^2 each)	Air-breathing, 2 layer of (CF sheet/ $K_3[Fe(CN)_6]$/PLL/ **BOD**) (1 cm^2 each)	0.1 M, 7 pH, (PBS), room temperature, 0.4 M **glucose**. Electrodes stacked with cellophane membrane in a single assembly.	1.45	0.3 V	0.8	SCC = 11 mA cm^{-2}.	Sakai et al. (2009)
CDH / polyvinylpyridine- Os complex/SWCNTs on graphite rods (3.05 mm diam.) with cross-linking	**Pt** –C (area ≫ anode area)	PBS, 7.4 pH, 37 °C, 0.1 M **glucose**, O_2 purged, non-quiescent	0.157	0.28 V	0.5		Tasca et al. (2008b)
PLL-K_3/diaphorase/**GDH** on GC (0.07 cm^2)	Poly-dimethylsiloxane coated **Pt** cathode	PBS, 7 pH, 5 mM **glucose**, 1 mM NAD^+, 37 °C	0.032	0.29 V	0.55	Current drops to half initial value after 18 h	Togo et al. (2007)
AlcDH/ AldDH / NAD^+/ modified Nafion on polymethylene green anode	**BOD** /modified Nafion on 1 cm^2 CF paper. Dried then soaked in $Ru(bpy)_3{}^{2+}$ mediator	7.15 pH, PBS, 1 mM **ethanol**, 1 mM NAD^+, room temperature	0.39, 0.83 (with Nafion membrane)	–	0.51, 0.68 (with Nafion)	Power increases to a maximum of 0.46 mW cm^{-2} then rapidly drops after 20 days.	Topcagic and Minteer (2006)
LDH /modified Nafion with $CaCl_2$ on CF paper (1 cm^2)	**Pt** –C black	Anolyte: 7.15 pH, PBS, 25 mM **lactate**. Catholyte: 1 M NaCl, dissolved O_2, 20 °C. Nafion Separator	0.022	–	0.85	Testing over 45 days without any claimed degradation in performance	Treu and Minteer (2008)
Porous Si-functionalised SWCNT-**GOx**	Porous Si-functionalised SWCNT-**laccase**	PBS, 4 mM **glucose**, air bubbling, stirred. 5 mm inter-electrode distance	1.38×10^{-3}	99 mV	–	Lower power density (0.35×19^{-3} mW cm^{-2}) at higher voltage (0.357 V) when SWCNTs grown by chemical deposition followed by carboxyl group attachment rather then electrophoretic deposition of pre-functionalised SWCNTs.	Wang et al. (2009)
Covalently linked SWCNT-NAD^+ deposited on classy carbon. **AlcDH** attached to NAD^+ through affinity, and cross-linked	Thioanaline modified **BOD** copolymerized with thioanaline capped **Pt** nanoparticles on Au electrode with thioanaline monolayer with crosslinking.	0.1 M PBS, 7 pH, 40 mM **ethanol** l, O_2 saturated	0.2	$0.55^{\dagger}$ V	0.62	Maximum power at 0.37 mA cm^{-2}	Yan et al. (2009)
GOx / MWCNTs/Nafion on carbon felt (0.33 cm^2)	Air-breathing **Pt** cathode	100 mM **glucose**, 10 mM 1.4-benzoquinone. Nafion/electrode assembly	0.077	0.51 V	0.57	–	Zheng et al. (2008)

[†] Values not explicitly reported, but estimated from graphical results.

the porosity; the chemical and mechanical stability of the gel; and negligible swelling (Lin and Brown, 1997; Wang, 1999).

A method to co-immobilise the enzyme and mediator (designed to prevent mediator leaching) was developed by Heller and co-workers, who used soluble redox hydrogels to construct biosensors and, subsequently, miniature biofuel cells (Chen et al., 2001; Mano et al., 2002b; Soukharev et al., 2004; Heller, 2004, 2006). In this method the enzyme is complexed with a redox polyelectrolyte forming a water soluble adduct, which is cross-linked on the electrode surface. The cross-linked polymer swells on contact with water to form a hydrogel, to which the enzymes are covalently bound. The enzymes are electrically connected to the electrode by a redox network and are said to be 'wired'; electron conduction is predominantly controlled by collisional electron transfer between the reduced and oxidized (transition metal-based) redox centers tethered to the polymer backbone. Popular choices for the polymer backbone are polyvinylimidazole, polyallylamine and polyvinylpyridine (PVP) and the redox centres are typically osmium (Os) or ruthenium complexes (Gregg and Heller, 1991). Os complexes are particularly useful due to the ease with which the redox potential can be tuned by chemical modification of the complex (Kavanagh et al., 2009). They can be tethered flexibly to polymer backbones, improving the electron transfer kinetics between the enzyme and electrode (Stoica et al., 2009). The mechanical strength of the hydrogels and the electron transfer rate can be improved by using spacers that connect the redox-active centers to the cross-linked networks. These spacers provide additional flexibility and improved collisional electron transfer. The lengths of the spacers are important; optimally between 8 and 15 atoms (Heller, 2006; Mano et al., 2005; Mao et al., 2003). The redox potentials of the hydrogels are determined by the transition metal ion of their complex and by its ligands, so they can be tailored to a specific enzyme/reaction combination (Heller, 2006; Kim et al., 2003). An example of a redox polymer structure, developed by Mao et al. (2003), is given in Fig. 3(a). The authors tethered a tris-dialkylated N,N′-biimidazole $Os^{2+/3+}$ complex to the backbone of a PVP polymer via 13-atom spacers. An order of magnitude increase in the apparent electron diffusion coefficient was observed when compared to a structure without spacers, used earlier by the authors. Furthermore, oxidation of glucose was found to occur at potentials close to the reversible potential of the FAD/$FADH_2$ centers of the enzyme.

Realising DET using GOx is difficult due to the deeply embedded nature of the active FAD sites. The same applies for PQQ and heme containing enzymes. In an attempt to overcome this issue, Willner and co-workers introduced a method based on reconstituting apo-enzymes on functionalised electrodes (Willner et al., 1996, 1998a,b; Xiao et al., 2003) (see Fig. 3(b) for an illustration). In one example, gold nanoparticles were linked to a gold electrode by a dithiol bridge, while amino-FAD was linked to the particles (Xiao et al., 2003). The FAD cofactor units were extracted from GOx to give the apo-enzyme, which was reconstituted on the FAD-functionalised particles. The gold nanoparticles were seen to act as electron relays between the FAD redox site and the electrode. Similarly, PQQ-dependent GDH was electrically wired by the reconstitution of apo-GDH on PQQ-functionalised nanoparticles (Zayats et al., 2005). Patolsky et al. (2004) instead reconstituted apo-GOx on FAD units linked to the ends of single wall carbon nanotubes (SWCNTs) assembled on a gold electrode, motivated by the efficient DET between SWCNTs and absorbed GOx redox active sites (Guiseppi-Elie et al., 2002; Cai and Chen, 2004). The authors deduced that the SWCNTs behaved as electrical contacts between the active site of the enzyme and the electrode. Such electrodes, using either single-walled or multi-walled CNTs (Ivnitski et al., 2006; Zhang et al., 2003) display good stability and sensitivity (Cai and Chen, 2004; Wang et al., 2003; Lin et al., 2004).

A summary of recent key developments in EFCs are presented in Table 1. They are discussed in detail in the sequel.

7.1. Physical immobilisation of enzymes and mediators

Tasca et al. (2008a) investigated the direct electron transfer (DET) capabilities of different CDHs adsorbed on a graphite electrode in the presence or absence of SWCNTs. SWCNTs were found to increase the electrocatalytic current, the onset of which was shifted to more negative potentials. CDH is composed of a large flavin-associated domain and a smaller heme-binding domain that allows direct electron transfer to the electrode. A membrane-less fuel cell was constructed using *Phanerochaete sordida* CDH coadsorbed with SWCNTs, together with a Pt/C cathode. A solution with 0.1 M, 4.5 pH citrate buffer containing O_2 and 5 mM lactose was used. The open circuit voltage was 590 mV and a maximum power density of 0.032 mW cm^{-2} at 430 mV was obtained. CDH was also adsorbed on graphite in a fuel cell with laccase immobilized in a polymer (Coman et al., 2008). The power density (0.005 mW cm^{-2}) was lower than the SWCNT system of Tasca et al. (2008a), but the cell voltages achieved were slightly higher.

In a similar fashion to CDH, FDH contains a heme group that should in principle allow direct electron transfer to the electrode. Previous investigations, however, were not successful in achieving practical currents. Kamitaka et al. (2007) immobilized FDH from *Gluconobacter* sp. by adsorption on a Ketjen's black (KB) modified carbon-paper anode that was capable of 4 mA cm^{-2}. Combined with a laccase biocatalyst from *Trametes* sp. adsorbed on a carbon aerogel cathode, a membrane-less bio-fuel cell was constructed and operated at room temperature in an O_2 saturated, 5 pH McIlvaine buffer containing 200 mM fructose. Under stirred conditions, to alleviate the O_2 mass transfer limitation, a maximum power density of 0.85 mW cm^{-2} at 410 mV was obtained and the open circuit voltage was recorded as 790 mV. The power output decreased to 63% of the maximum after 12 h of continuous operation. Under low power conditions, 4 cells connected in series continuously powered a small light-emitting diode for 60 days. Since the cell was operated at low power output for two months, the short lifetime was unlikely to be due to enzyme desorption but rather to a loss of activity during continuous operation at a high current density.

Though stirring is not usually desired in real applications, it is often used in systems to improve mass transport and increase the power output. Katz et al. (2005) investigated the effects of a constant magnetic field applied parallel to the electrode surface in surface-confined bio-electrocatalytic systems. In the two systems of GOx-FAD-PQQ and lactate dehydrogenase (LDH)/NAD^+-PQQ, in which the current was limited by mass transport, it was found that the current increased by a factor of three when a magnetic field (0.92 T) was applied. This improvement was brought on by a magnetohydrodynamic effect, engendering a magnetic force on the ions in solution, and thus decreasing the hydrodynamic layer thickness and increasing the current density.

Glucose dehydrogenase (GDH) was later immobilized with its cofactor, NAD^+ on KB, supported on a GC rod (Miyake et al., 2009). Together with a BOD/KB cathode, the constructed fuel cell was operated in an O_2 saturated phosphate buffer solution (PBS) containing 50 mM glucose. It achieved a maximum power density of 0.052 mW cm^{-2} at 0.3 V with an open circuit voltage (OCV) of 0.642 V.

Physical adsorption is attractive due to its simplicity, although enzyme retention is usually problematic. A review of systems employing simple adsorption shows that, despite exhibiting 'normal' cell voltages, they have low power densities compared to alternative systems based on the same biocatalysts. This indicates either poor electron transport despite the direct capabilities, or is possibly a result of the low maximum enzyme loadings that can be achieved.

7.2. Enzyme immobilisation in polymers

Early hydrogel-modified electrodes in EFCs performed well over a period of a few days but suffered long-term stability issues (Calabrese-Barton et al., 2004). Amongst the causes of lost activity were (a) leaching of components from the cross-linked matrix and (b) hydrogel loss (Binyamin and Heller, 1999; Boland et al., 2009b). A recently developed method for improving stability consists of anchoring the hydrogel to the electrode surface via covalently attached tether groups (Boland et al., 2009b; Lehr et al., 2010). Boland et al. (2009b) compared the current densities and stabilities of pre-treated and bare graphite and Au electrodes. The pre-treated graphite electrodes were functionalised to yield the amine functional groups by electrochemical reduction of a diazonium salt from 1,4-phenylenediamine. An Os-based redox polymer was then cross-linked on the bare and pre-treated electrodes, with GOx on the anode and BOD on the cathode. For both electrodes, retention of activity was vastly improved by pre-treatment, although the test times of 48 h were still rather short. The authors postulated that the improved stability was due to the presence of amine groups on the pre-treated surfaces; these groups are amenable to anchoring of the hydrogel through reaction with the oxirane ring of the crosslinker.

Recently, Sakai et al. (2009) prepared an anode by successively applying solutions of poly-L-lysine (PLL), GDH, diaphorase, NADH, vitamin K_3 and polyacrylic acid sodium salt to four separate carbon fiber (CF) sheets. A membrane electrode assembly (MEA) was constructed by combining the anode with a cellophane membrane and an air-breathing cathode, fabricated by successively treating two CF sheets with $K_3[Fe(CN)_6]$, PLL and BOD solutions. A bio-fuel cell containing the MEA and a 0.1 M, 7 pH PBS at room temperature with 0.4 M glucose yielded a power density of 1.45 mW cm^{-2} at 0.3 V with an OCV of 0.8 V and a short circuit current (SCC) of 11 mA cm^{-2}. The diaphorase biocatalyst was used for a reduced overpotential oxidation of NADH with vitamin K_3 as the electron mediator. Two cells were then connected in series to operate a small toy car (16.5 g) for more than 2 h continuously. The assembled unit had a power output of 100 mW, a volume of 80 cm^3, and a weight of 39.7 g, of which 16.1 g was the fuel solution.

LDH is one of the many PQQ dependent enzymes capable of DET through a heme group (Treu and Minteer, 2008). Treu and Minteer (2008) isolated PQQ-dependent LDH bound to the outer membrane of *Gluconobacter* and purified them through ion exchange chromatography. The enzyme was immobilized with a tetrabutylammoniumbromide (TBAB)-modified Nafion solution on CF paper. $CaCl_2$ was also used in the immobilization since Ca^{2+} ions are used to coordinate the PQQ cofactor with the apoenzyme. The anode was combined with a Pt cathode and a Nafion membrane.

Khani et al. (2006) explored the use of alginate polymer beads in a low cost, simple method for enhanced enzyme retention. It was found that the use of pure alginate or alginate/carbon beads for the immobilization of GOx and laccase maintained 75% and 91% of the enzymatic activities, respectively, and doubled the active half-life of the enzymes. The rates of activity loss for entrapped laccase and BOD were 0.6% and 1.14% per day, respectively. While the turnover rate of GOx improved with the alginate beads (compared to a solution), the opposite was true for laccase. The Michaelis–Menten constant for GOx in the alginate beads increased by almost a factor of four, an effect that was explained by the limited substrate concentration near the enzymes.

Polymers containing redox mediator metal complexes have been used in the immobilization of GOx (Mano et al., 2005; Mano, 2008; Gao et al., 2009), lacasse (Calabrese-Barton et al., 2001; Soukharev et al., 2004; Barriere et al., 2004; Gallaway and Calabrese Barton, 2008) and BOD (Mano et al., 2002a). Mano (2008) used Os based metal complexes attached to a PVP polymer in addition to a crosslinking agent to wire GOx and laccase to two 7 μm diameter ×2 cm long GC electrodes. The GOx was sourced from *P. pinophilum* rather than the traditional *Aspergillus niger* since it has a lower Michaelis constant (which is needed for operating the miniature fuel cell in a glucose concentration similar to that found in physiological conditions, 5–8 mM). In a 20 mM citrate buffer with 5 mM glucose at 5 pH (optimum for GOx) and 37 °C, the fuel cell was capable of producing 0.28 mW cm^{-2} at 0.88 V, and operated continuously for 1 month at a power loss of 3% per day for the first 2 weeks. At neutral pH, however, *Penicillium pinophilum* is unstable and denaturation of the enzyme was found to occur; the optimum pH was in the range 4–6.

Gao et al. (2009) investigated the performance of different polymer backbones and a 7.24 pH PBS, GOx from *A. niger*, containing 15 mM glucose and atmospheric O_2. The main purpose of this study was to investigate the effect of purifying the enzyme. Commercial enzyme stocks usually contain other chemical elements whose exact composition is unknown. Purification of the stock was found to improve the specific activity and the performance of a fuel cell compared to non-purified enzymes.

Organic polymers have also been used to covalently attach enzymes. In the work by Kuwahara et al. (2009), 3-methylthiophene and thiophene-3-acetic acid were copolymerised into a film on a gold coated alumina plate. Subsequently, GOx and BOD were covalently attached to the carboxyl groups of the polymer. Appropriate mediators were used in the two PBS (7 pH) solutions separated by a Nafion membrane. The anolyte was saturated with nitrogen and contained 0.1 M glucose while the catholyte was saturated with O_2. The OCV and maximum current density, both higher with BOD/copolymer than with Pt/C cathodes, were 0.61 V and 0.15 mW cm^{-2} at 0.35 V. Periodic measurements of the separate half-cell currents showed that the anodic current decreased by 50% over one month, while the cathodic current decreased by 25%.

Brunel et al. (2007) made a membrane-less bio-fuel cell using porous tubes supplied internally with O_2 and containing the biocatalyst at the outer surfaces exposed to the anolyte. GOx and its mediator, 8-hydroxyquinoline-5-sulfonic (HQS) acid, were co-immobilized in polypyrrole (PPy) polymer and the cathode was similarly prepared using laccase and its mediator, 2,2′-azinobis (3-ethylbenzothiazoline-6-sulfonate) diammonium salt (ABTS), on a porous carbon tube. A solution of nitrogen saturated PBS and 10 mM glucose at 37 ° C was used. A separate solution containing dissolved O_2 was circulated inside the cathode. At a pH of 5, a maximum power density of 0.027 mW cm^{-2} at 0.24 V was obtained. This decreased to 0.020 mW cm^{-2} at 7 pH. Some degree of leakage of the ABTS mediator was observed. The cell was tested intermittently after being stored at 4 ° C and retained 80% of its initial power density after 1 month.

Tamaki and Yamaguchi (2006) have immobilised a quinone mediator on a flexible spacer to polymer grafted on carbon black (Tamaki and Yamaguchi, 2006; Tamaki et al., 2007). The electrode was then immersed in GOx solution, and a cross-linking agent was applied after drying. The aim was to create a three-dimensional structure where the electron conduction was divided between the carbon particles and the redox polymers.

The DET of GOx has been established using a simple anode fabrication method and without the use of nanomaterials. In the work by Wang and Chen (2009), GOx was immobilized in PLL on a GC electrode, before a layer of Nafion was applied. Electrochemical tests on the Nafion-PLL-GOx anode showed reversible electrochemical behavior of the GOx and a performance similar to that using nanomaterials.

Rather than using polymers applied as films, Kim et al. (2009) prepared an anode using PPy nanowires to immobilize GOx and its mediator, HQS, on a nanoporous anodized aluminum oxide electrode. Different nanowire lengths, diameters, and electrode base preparation methods were tested, along with a single cathode made by immobilizing a mixture of laccase and its mediator, ABTS, in a PPy film on a gold electrode. With increasing nanowire length, the cell showed a decrease in OCV and an increase in the power density, which reached 0.28 mW cm^{-2} (at 0.15 V) using a 200 nm diameter ×16 μm length wire. This system suffered from low operating and open-circuit cell voltages, probably due to the high resistance of the long nanowires. The voltage was found to increase using 350 nm long wires grown directly on the Au surface, but the current and power output would be expected to decrease due to a decrease in the available surface area for enzyme immobilization.

7.3. Reconstructed apoenzymes and sol–gels

Monolayers of enzymes covalently bonded through redox relay molecules have been used for the construction of anodes (Zayats et al., 2008, and references therein). Lee et al. (2009) attached NAD$^+$-dependent LDH to PQQ electron mediators, which were in turn attached to a gold electrode by a cystamine monolayer. The novelty of the method introduced was that the final step of covalent attachment of LDH was performed in the presence of the NAD$^+$ cofactor, lactate substrate, and Ca^{2+}, which helped to promote a favorable orientation of the LDH after immobilization. The bioelectrochemical oxidation reactions of NADH, mediated by PQQ and leading to an electron transfer to the anode are (Shukla et al., 2004):

$$\mathrm{NADH} + \mathrm{PQQ} + \mathrm{H}^+ \rightarrow \mathrm{NAD}^+ + \mathrm{PQQH}_2 \tag{4}$$

$$\mathrm{PQQH}_2 \rightarrow \mathrm{PQQ} + 2\,\mathrm{H}^+ + 2\,\mathrm{e}^-\ (\text{to anode}) \tag{5}$$

The anode was combined with a cathode composed of microperoxidase (MP-11) attached to a monolayer of cystamine on a gold electrode. The anolyte consisted of 0.1 M, 7 pH, tris buffer containing optimized solution concentrations of 10 mM CaCl$_2$, 10 mM NAD$^+$ and 5 M lactate, while the catholyte consisted of a 0.1 M, 7 pH, PBS containing 1 mM hydrogen peroxide as the electron acceptor and ABTS as the mediator. The two compartments were separated by a Nafion membrane and the cell was operated at room temperature. The maximum power density obtained was 0.142 mW cm^{-2}. No mention was made of the cell voltage but a reading from the power and polarization plots shows that the OCV was around 0.34 V, and the maximum power density was achieved at around 0.1 V; relatively low when compared to the difference in the formal potential of the two mediators, 0.585 V ($E^0_{\mathrm{ABTS}} = 0.46$ (Zebda et al., 2009b) and $E^0_{\mathrm{PQQ}} = -0.125$ (Katz et al., 1999a)).

Sol–gel was employed by Lim et al. (2007) for the encapsulation of GOx, using tetramethoxy silane as the precursor for the silica gel incorporating both the biocatalysts (GOx and BOD) and SWCNTs. Ferrocene methanol and ABTS were the mediators in the membrane-separated anodic and cathodic compartments, respectively. Both compartments contained phosphate buffer solutions, with 100 mM of glucose at the anode side and saturated O$_2$ at the cathode side. Operating at room temperature, the fuel cell achieved a maximum power density of 0.120 mW cm^{-2} at 0.24 V, with an OCV of 0.48 V. Immobilization in a hydrogel removed any effects associated with orientation of the enzymes. Mobile enzymes diffuse in the gel, increasing the number of active enzymes and thus increasing the current, which may reach three times that for a monolayer (Tsujimura et al., 2005). The performance was poor when compared to other systems using the same biocatalysts and operating at a similar pH and fuel concentration.

7.4. Nanostructured electrodes

In recent years, the use of nanotechnology to develop biofuel cell electrodes has become widespread. Nano-structured materials have been shown to be appropriate hosts for enzyme immobilization, providing a greater surface area for attachment and improving enzyme kinetics (Kim et al., 2006). They can also be used as electrical 'wires' between the electrode and the active redox centre of the enzyme.

Lee et al. (2010) compared a fuel cell constructed using GOx and laccase with a cell containing SWCNT and a cell containing DNA-wrapped SWCNT. The use of single-stranded DNA-wrapped SWCNTs was found to increase the GOx loading to 73.3 μg mm^{-2} compared to approximately 19 μg mm^{-2} for both SWCNT/FAD-GOx and cystamine/PQQ/FAD-GOx anodes. The electron conductivity at the three anodes was also studied and the results showed that the two electrodes containing SWCNT had similar conductivities, which were an order of magnitude greater than that of the cystamine/PQQ/FAD-GOx anode. A membrane-less fuel cell employing DNA-wrapped SWCNTs for immobilization of GOx and laccase and operating in a PBS (7 pH, 25 °C) using glucose and O$_2$ (the fuel concentration was unspecified) achieved a maximum power density of 0.442 mW cm^{-2} at 0.46 V, with an OCV of approximately 1.5 V. The authors suggested that DNA wrapping contributes towards decreasing the shear stress between the enzyme and the SWCNT, in addition to acting as the primary electron transfer mediator. These results are, however, questionable since the high OCV cannot be explained in terms of the redox potentials of the two biocatalysts ($E^0_{\mathrm{GOx}} \approx -0.34$ V and $E^0_{\mathrm{laccase}} \approx 0.54$ V *vs.* SCE (Zebda et al., 2009b)). The power density obtained using this pair of mediator-less biocatalysts was higher than those obtained with the same catalysts either entrapped in polymers with mediators (Brunel et al., 2007), or wired through mediator activated polymers (Mano, 2008). Moreover, this system (Lee et al., 2010) was operated at neutral pH, a condition that is not optimal for *Trametes versicolor* laccase activity.

These disadvantages of using laccase have been found to be source dependent. Those sourced from *Melanocarpus albomyces*, for instance, display optimum activity close to neutral conditions (Kavanagh et al., 2009). Kavanagh et al. immobilised laccase with an Os containing polymer, while the anode contained suspended, mediated GOx. The maximum power density was 0.052 mW cm^{-2} at 0.21 V with and OCV of 0.55 V. Ivnitski et al. (2006) prepared a GOx anode using multi-walled carbon nanotubes (MWCNTs), which were grown using cobalt nanoparticles deposited on a carbon paper (CP). A mixture of GOx and polyethyleneimine was then applied to the electrode, followed by a casting of Nafion. The positively charged polycation acts as a binder between the negatively charged GOx and the CP/MWCNT electrode.

Fischback et al. (2006) used enzymes in cross-linked clusters covalently immobilized on functionalised CNTs, which were than cast on a carbon felt. The preparation procedure involved immobilizing single GOx enzymes on functionalised CNTs, before adding ammonium sulfate to form enzyme clusters from the remaining freely suspended GOx. These clusters around the CNTs were then cross-linked and applied with Nafion on a carbon felt electrode. The anode was combined with a proton exchange membrane and an air-breathing Pt cathode. The cell was tested in the absence of a buffer, with an ammonium buffer and with a sodium buffer. In the absence of a buffer, the initial performance was poor, but the cell remained stable over a longer period of time and maintained almost constant power output. The maximum power density was 0.120 mW cm^{-2} at 0.1 V with an OCV of 0.33 V. The buffered cells underwent a degradation in performance due to the presence of cations, which hinder the passage of protons through the membrane. Cross-linked enzyme clusters have previously been shown by the same group to provide good stability and high activity retention (up to 250 days). While an un-buffered solution was found to give better performance due to a lack of interference with proton transport, it may also have led to the low operating voltage (low solution conductivity). The use of an alternative membrane in the buffered cells to alleviate the problem of hindered proton transport, while not increasing the internal resistance, was not investigated.

Deng et al. (2008) applied several coatings of AuNP/enzyme bilayers on macroporous gold electrodes initially treated with cystamine. Using GDH and laccase as enzymes, a membrane-less fuel cell was constructed. The cell was studied with respect to the number of bilayers and compared to one with flat gold electrodes and one bilayer. A maximum power density of 0.178 mW cm^{-2} at 226 mV was achieved using five bilayers while the OCV was 0.32 mV. The current and power density were found to increase with the first 5 layers and in all cases were higher than with flat electrodes. A higher OCV (0.52 V) was observed with flat gold electrodes, and was attributed by the authors to a difference in the O_2 reduction potential compared to that for the macroporous cathode. However, CVs of these two anodes showed that a current peak occurred at a slightly higher potential with the flat electrode, indicating that the lower cell voltage is due to both electrode potentials, possibly as a consequence of the higher electrical resistance of the macroporous materials.

SWCNTs on GC have been used to attach AlcDH to covalently linked NAD$^+$ (Yan et al., 2009). This anode was combined with a cathode containing both Pt and BOD in a copolymer cross-linked matrix and the cell was operated with 0.1 M PBS and 40 mM of ethanol at a pH of 7.0 (Fig. 4). A maximum power density of 0.2 mW cm^{-2} at 0.55 V and 0.37 mA cm^{-2} with an OCV of 0.62 V were attained. While CNTs are employed for their good conductivity and large surface area for depositing the enzymes, Zhou et al. (2009) showed that a higher voltage and power density can be obtained with a mesoporous carbon based material.

Ideally, enzymatic electrodes for power generation should maximize enzyme loading, activity and stability, while also minimizing inefficiencies due to substrate mass transport limitations and slow electron transfer from the enzyme to the electrode. While increasing bond strength (physical adsorption/entrapment, ionic bonding, and covalent bonding) improves enzyme retention, deactivation is also more probable (Sheldon, 2007). Simple physical binding or entrapment in polymers is sometimes complemented by ionic binding, but this imposes an operating pH depending on the type of enzyme used and the ionomer charge. Addition of a cross-linking agent is a simple and widely used method to improve the stability and increase both the concentration of the enzyme and its activity (Sheldon, 2007).

The random enzyme orientation, when physically adsorbed or covalently bonded, is unfavourable for efficient electron communication with the active site. The reconstruction of apo-enzymes around the active site bound to a redox relay provides excellent electrical communication. Monolayers of these electrically contacted enzymes have a high turnover number and sensitivity, although the enzyme loading is limited by the electrode surface area. This limitation can be relieved by a similar enzyme reconstitution but on an electrically active thin polymer film (Zayats et al., 2008). Immobilization of mediators and enzymes on polymer films is a simple and practical method for biofuel cell electrodes; however, the effective diffusion coefficient of the mediator (and hence the electron transport rate) is several orders of magnitude lower than that of a typical diffusional mediator (Kim et al., 2006).

The increasing use of nanostructures (such as nanoparticles, nanofibers and CNTs) has a twofold advantage: providing a greater surface area for the biocatalysts and enhancing their stability and activity (Kim et al., 2008). These procedures are, on the other hand, relatively costly. Some reports have claimed that CNTs can have an adverse effects on the enzyme kinetics (Zhao et al., 2009), indicating that the use of these structures requires a careful selection of enzymes, electrode materials and attachment methods. More generally, a careful optimization of the nanostructure size is required, since small pores can lead to mass transport limitations for the mediator/substrate and large pores can lead to leaching of the enzyme (Kim et al., 2006).

7.5. *Fuel oxidation*

In many enzymatic fuel cells, both the cathode and anode are enzyme-based, with the aim of combining the benefits of higher stability and the good catalytic activity of inorganic materials, together with improved O_2 reduction kinetics via biocatalysts at low temperatures (Choi et al., 2009; Habrioux et al., 2007, 2009). Habrioux et al. (2009) used Au–Pt nanoparticles supported in a Nafion/carbon-black mix, together with BOD and its mediator ABTS co-immobilized in a Nafion film to construct a concentric bio-fuel cell. A maximum power density of 0.19 mW cm^{-2} at 0.52 V was achieved at 37 ° C and 7.4 pH using 0.7 M glucose. An appreciable power density of 0.09 mW cm^{-2} could still be achieved at a lower glucose concentration of 10 mM.

Most fuels used in EFCs are either saccharides, such as glucose, lactose, fructose and cellobiose, or alcohols such as ethanol. Recently, glycerol has been considered due to its high energy density and abundance (it is a byproduct of biodiesel) (Arechederra et al., 2007; Arechederra and Minteer, 2009). In a study by Arechederra et al. (2007), a cascade of two PQQ-dependent enzymes, AlcDH and aldehyde dehydrogenase (AldDH) was immobilized in modified Nafion on a CP/Pt cathode, and the assembled fuel cell produced a maximum power density of up to 1.21 mW cm^{-2}. This cell was further developed by adding a third enzyme, oxalate oxidase (Arechederra and Minteer, 2009), which allowed the complete oxidation of glycerol and slightly increased the maximum power density to 1.32 mW cm^{-2} with 100 mM of glycerol. However, the cell was less tolerant to high fuel concentrations compared to the original cell.

Another enzyme cascade system was reported by Topcagic and Minteer (2006). Ethanol was oxidized to acetate by AlcDH and AldDH and dissolved O_2 was reduced by BOD immobilized with two consecutive mediators in Nafion. In a membrane-less system employing 7.15 pH PBS with 1 mM ethanol and 1 mM NAD$^+$ as the anodic mediator, an OCV of 0.51 V and a maximum power density of 0.39 mW cm^{-2} were achieved. Both the voltage and power were lower than an equivalent cell employing a Nafion membrane separator. Ramanavicius et al. (2008) developed a fuel cell that used ethanol as the substrate for both half reactions, with an AlcOD/MP cascade on the cathode and AlcDH on the anode. The maximum power density was 1.5×10^{-3} mW cm^{-2} with an OCV of 0.24 V.

In addition to the development of enzyme/electrode preparation methods, several studies have been aimed at optimising systems according to the buffer type and concentration, redox polymer composition, and binder-to-enzyme ratios (Sakai et al., 2009; Kjeang et al., 2006; Kontani et al., 2009; Mano et al., 2005; Stoica et al., 2009). Most of the choices were specific to the setup used and are of limited use for other designs. In the case of microfluidic fuel cells, numerical optimization of the channel dimensions has been performed by several groups (Zebda et al., 2009a,b; Togo et al., 2008).

Membrane-less fuel cells have several attractive features, including structural simplicity, reduced cost, and a greater scope for miniaturization. There are, however, several requirements for such systems: specificity of the two half reactions occurring, such that the substrates/products of one do not interfere with the other, and acceptable operating conditions common to both biocatalysts (Stoica et al., 2009). A number of membrane-less systems have been

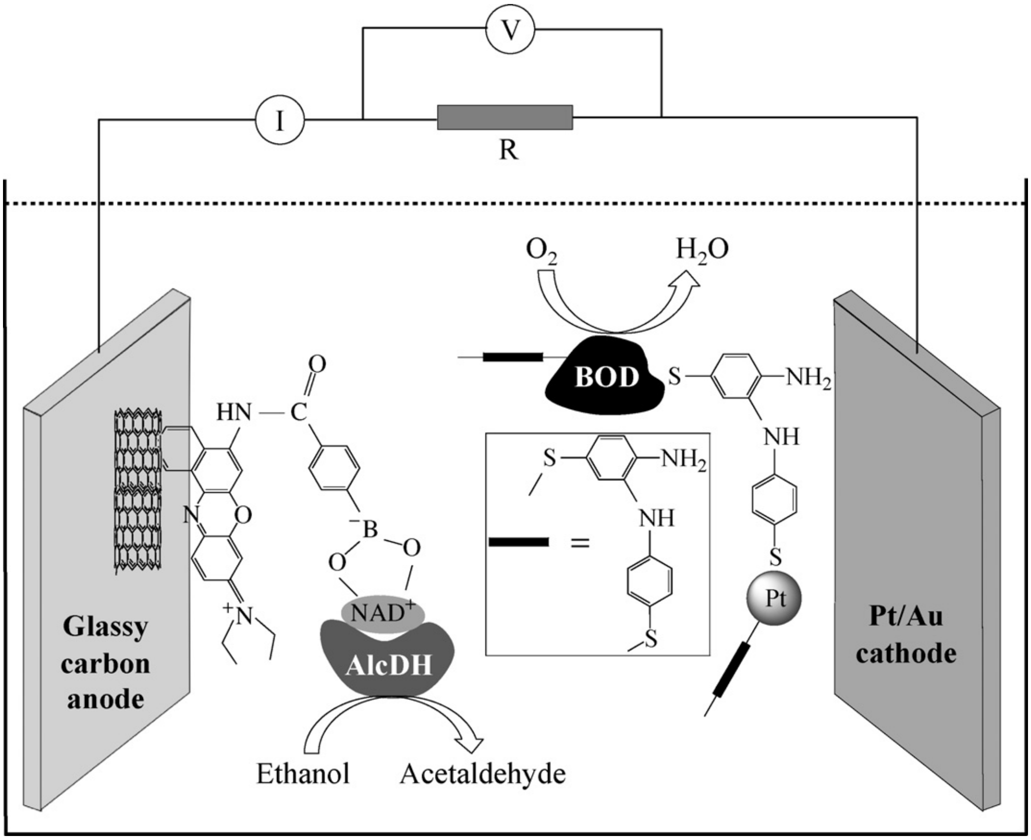

Fig. 4. A schematic representation of a membrane-less bio-fuel cell employing bioelectrocatalytic electrodes composed of (a) alcohol dehydrogenase (AlcDH) reconstituted on a relay-NAD^+ monolayer associated with carbon nanotubes (anode); and (b) a platinum-nanoparticle/bilirubin-oxidase (BOD) crosslinked composite on a Au/Pt electrode (cathode). Adapted from Yan et al. (2009).

developed, exhibiting varying degrees of electrical performance. In systems based on DET using CDH/laccase (Coman et al., 2008), CDH/BOD (Coman et al., 2009), or GOx/laccase (Wang et al., 2009), power densities of only a few μW cm^{-2} have been realised. The first two systems employing CDH exhibited relatively high operating and open cell voltages, and hence the low power was due to a low current, specifically the anodic current. This was potentially due to unfavorable orientation of CDH after immobilization; CDM has one FAD domain and one heme domain allowing DET to the electrode. Membrane-less systems employing mediators, and either GDH/BOD (Gao et al., 2007), AlcDH/BOD (Topcagic and Minteer, 2006), GDH/laccase (Deng et al., 2008), or FDH/laccase (Kamitaka et al., 2007), can have power densities 1–2 orders of magnitude higher than those yielded by DET. The absence of soluble mediators, however, remains an essential feature of the flow type fuel cells proposed for *in vivo* applications.

8. Summary and outlook

In the last few years, enzymatic fuel cells have approached power densities of ~1 mW cm^{-2}. For portable electronic applications, high energy density fuels such as ethanol (Topcagic and Minteer, 2006) and glycerol (Arechederra and Minteer, 2009) show great promise. Developments in the overall system design have also led to more efficient systems. For example, removing the separator membrane without significant loss in power output, and the emergence of single chamber, air-breathing systems using compact MEAs. For many proposed applications, however, further substantial improvements in performance are required (higher power densities and energy efficiencies).

For both MFC and EFC, electrode materials need to be more catalytic while maintaining their performance, particularly in the face of problems caused by fouling of the active surfaces and loss of enzyme activity. It is also important to study time-dependent performance over practical periods, particularly with a focus on long-term changes in the enzyme activity.

A greater understanding and characterisation of the reaction environment can be achieved through studies of the reactant and charge distribution, mass transport and mass transfer, as well as the bio-electrochemical reaction kinetics. Carefully validated models can be used in conjunction with laboratory studies to investigate these processes (particularly *in situ*) and to accelerate the development of practical systems. To date, only a small number of models have been developed for specific systems (Bartlett and Pratt, 1995; Kano and Ikeda, 2000; Ikeda and Kano, 2001; Gallaway and Calabrese Barton, 2008; Calabrese-Barton, 2005; Kjeang et al., 2006; Zeng et al., 2010; Marcus et al., 2007; Picioreanu et al., 2007, 2010). Models for other electrochemical cells, including polymer electrolyte membrane (PEM) fuel cells and batteries (Shah and Walsh, 2008; Shah et al., 2009, 2008) are ideal templates for further developing BFC models.

A vitally important aspect of bio-fuel cell performance and stability is the immobilization of the enzyme/mediator on the electrode. Maintaining a continuous supply of fuel to the active sites and ensuring an efficient electron-transfer process from the enzyme/bacteria to the electrode via the mediator are crucial. While previous research was mainly targeted at developing the enzyme chemistries (Bullen et al., 2006), the past 5 years can be marked by efforts to develop new methods and materials for integrated enzyme electrodes that maximize enzyme loading and move from the classic two-dimensional loading to highly ordered three-dimensional structures with improved enzyme stabilization (Kim et al., 2008). These use of nanostructures shows great promise, though it should be kept in mind that for application purposes the materials must be safe and cost effective, and the fabrication techniques must be practical.

From an engineering perspective, cells with chemistries that allow single-compartment operation and possess constructional simplicity would be highly advantageous. It is important that low-cost, modular and scalable designs are developed, particularly if they are to form the basis for multi-plate (e.g. bipolar) cell stacks. At the present time, there are very few examples of BFC stacks (Aelterman et al., 2006; Sakai et al., 2009). In this respect, much could be learned from the rapid progress in PEM fuel cell MEA/stack performance over the past two decades (Barbir, 2005). Cell construction has been improved to optimise the cell voltage through comprehensive modelling/experimental studies of the electrode overpotentials and all cell resistances; there is a vast body of literature on the electrical, thermal, transport and mechanical properties of electrode, plate and membrane materials.

References

Aelterman, P., Rabaey, K., Pham, H.T., Boon, N., Verstraete, W., 2006. Environ. Sci. Technol. 40, 3388–3394.
Allongue, P., Delamar, M., Desbat, B., Fagebaume, O., Hitmi, R., Pinson, J., Savéant, J.M., 1997. J. Am. Chem. Soc. 119, 201–207.
Arechederra, R.L., Boehm, K., Minteer, S.D., 2009. Electrochim. Acta 54, 7268–7273.
Arechederra, R.L., Minteer, S.D., 2009. Fuel Cells 9, 63–69.
Arechederra, R.L., Treu, B.L., Minteer, S.D., 2007. J. Power Sources 173, 156–161.
Barbir, F., 2005. PEM Fuel Cells: Theory and Practice. Elsevier/Academic Press, London.
Barriere, F., Ferry, Y., Rochefort, D., Leech, D., 2004. Electrochem. Commun. 237, 237–241.
Bartlett, P.N., Pratt, K.F.E., 1995. J. Electroanal. Chem. 397, 61–78.
Binyamin, G., Heller, A., 1999. J. Electrochem. Soc. 146, 2965–2967.
Boder, E.T., Wittrup, K.D., 1997. Nat. Biotechnol. 15, 553–557.
Boland, S., Foster, K., Leech, D., 2009a. Electrochim. Acta 54, 1986–1991.
Boland, S., Jenkins, P., Kavanagh, P., Leech, D., 2009b. J. Electroanal. Chem. 626, 111–115.
Brooksby, P.A., Downward, A.J., 2004. Langmuir 20, 5038–5045.
Brunel, L., Denele, J., Servat, K., Kokoh, K.B., Jolivalt, C., Innocent, C., Cretin, M., Rolland, M., Tingry, S., 2007. Electrochem. Commun. 9, 331–336.
Bullen, R.A., Arnot, T.C., Lakeman, J.B., Walsh, F.C., 2006. Biosens. Bioelectron. 21, 2015–2045.
Cai, C., Chen, J., 2004. Anal. Biochem. 332, 75–83.
Calabrese-Barton, S., 2005. Electrochim. Acta 50, 2145–2153.
Calabrese-Barton, S., Kim, H.H., Binyamin, G., Zhang, Y.C., Heller, A., 2001. J. Am. Chem. Soc. 123, 5802–5803.
Calabrese-Barton, S.A., Gallaway, J.W., Atanassov, P., 2004. Chem. Rev. 104, 4867–4886.
Call, D., Logan, B.E., 2008. Environ. Sci. Technol. 42, 3401–3406.
Cao, L., 2005. Curr. Opin. Biotechnol. 9, 217–226.
Cao, X., Huang, X., Boon, N., Liang, P., Fan, M., 2008. Electrochem. Commun. 10, 1392–1395.
Chen, T., Calabrese-Barton, S., Binyamin, G., Gao, Z., Zhang, Y., Kim, H.H., Heller, A., 2001. J. Am. Chem. Soc. 123, 8630–8631.
Cheng, S., Xing, D., Call, D.F., Logan, B.E., 2009. Environ. Sci. Technol. 43, 3953–3958.
Cho, Y.K., Donohue, T.J., Tejedor, I., Anderson, M.A., McMahon, K.D., Noguera, D.R., 2008. J. Appl. Microbiol. 104, 640–650.
Choi, Y., Wang, G., Nayfeh, M.H., Tung Yau, S., 2009. Biosens. Bioelectron. 24, 3103–3107.
Clauwaert, P., Aelterman, P., Pham, T.H., De Schamphelaire, L., Carballa, M., Rabaey, K., Verstraete, W., 2008. Appl. Microbiol. Biotechnol. 79, 901–913.
Coman, V., Ludwig, R., Harreither, W., Haltrich, D., Gorton, L., Ruzgas, T., Shleev, S., 2009. Fuel Cells 10, 9–16.
Coman, V., Vaz-Domínguez, C., Ludwig, R., Harreither, W., Haltrich, D., DeLacey, A., Ruzgas, T., Gorton, L., Shleev, S., 2008. Phys. Chem. Chem. Phys. 10, 6093–6096.
Cooney, M.J., Svoboda, V., Lau, C., Martin, G., Minteer, S.D., 2008. Energy Environ. Sci. 1, 320–337.
Davis, F., Higson, S.P.J., 2007. Biosens. Bioelectron. 22, 1224–1235.
Delamarche, E., Michel, B., Kang, H., Gerber, C., 1994. Langmuir 10, 4103–4108.
Deng, L., Wang, F., Chen, H., Shang, L., Wang, L., Wang, T., Dong, S., 2008. Biosens. Bioelectron. 24, 329–333.
Dubois, L.H., Nuzzo, R.G., 1992. Ann. Rev. Phys. Chem. 43, 437–463.
Ferapontova, E.E., Ruzgas, T., Gorton, L., 2003. Anal. Chem. 75, 4841–4850.
Fischback, M.B., Youn, J.K., Zhao, X., Wang, P., Park, H.G., Chang, H.N., Kim, J., Ha, S., 2006. Electroanalysis 18, 2016–2022.
Fishilevich, S., Amir, L., Fridman, Y., Aharoni, A., Alfonta, L., 2009. J. Am. Chem. Soc. 131, 12052–12053.
Furukawa, Y., Moriuchi, T., Morishima, K., 2006. J. Micromech. Microeng. 16, 220–S225.
Gallaway, J.W., Calabrese Barton, S.A., 2008. J. Am. Chem. Soc. 130, 8527–8536.
Gao, F., Courjean, O., Mano, N., 2009. Biosens. Bioelectron. 25, 356–361.
Gao, F., Yan, Y., Su, L., Wang, L., Mao, L., 2007. Electrochem. Commun. 9, 989–996.
Ghindilis, A.L., Atanassov, P., Wilkins, E., 1997. Electroanalysis 9, 661–674.
Gooding, J.J., Hibbert, D.B., 1999. Trac-Trend Anal. Chem. 18, 525–533.
Gooding, J.J., Mearns, F., Yang, W., Liu, J., 2003. Electroanalysis 15, 81–96.
Gregg, B.A., Heller, A., 1991. J. Phys. Chem. 95, 5970–5975.
Guiseppi-Elie, A., Lei, C., Baughman, R.H., 2002. Nanotechnology 13, 559–564.
Habrioux, A., Servat, K., Tingry, S., Kokoh, K.B., 2009. Electrochem. Commun. 11, 111–113.
Habrioux, A., Sibert, E., Servat, K., Vogel, W., Kokoh, K., Alonso-Vante, N., 2007. J. Phys. Chem. B 111, 10329–10333.
Harper, A., Anderson, M.R., 2010. Sensors 10, 8248–8274.
He, Z., Angenent, L.T., 2006. Electroanalysis 18, 2009–2015.
He, Z., Kan, J., Mansfeld, F., Angenent, L.T., Nealson, K.H., 2009. Environ. Sci. Technol. 43, 1648–1654.
He, Z., Minteer, S.D., Angenent, L.T., 2005. Environ. Sci. Technol. 39, 5262–5267.
Heller, A., 1992. J. Phys. Chem. 96, 3579–3587.
Heller, A., 2004. Phys. Chem. Chem. Phys. 6, 209–216.
Heller, A., 2006. Curr. Opin. Chem. Biol. 10, 664–672.
Ikeda, T., Kano, K., 2001. J. Biosci. Bioeng. 92, 9–18.
Ishii, S., Shimoyama, T., Hotta, Y., Watanabe, K., 2008. BMC Microbiol. 8, 6.
Ishikawa, M., Yamamura, S., Takamura, Y., Sode, K., Tamiya, E., Tomiyama, M., 2006. Int. J. Hydrogen Energy 31, 1484–1489.
Ivnitski, D., Branch, B., Atanassov, P., Apblett, C., 2006. Electrochem. Commun. 8, 1204–1210.
Jang, J.K., Pham, T.H., Chang, I.S., Kang, K.H., Moon, H., Cho, K.S., Kim, B.H., 2004. Proc. Biochem. 39, 1007–1012.
Kamitaka, Y., Tsujimura, S., Setoyama, N., Kajino, T., Kano, K., 2007. Phys. Chem. Chem. Phys. 9, 1793–1801.
Kandimalla, V.B., Tripathi, V.S., Ju, H.X., 2006. Crit. Rev. Anal. Chem. 36, 73–106.
Kano, K., Ikeda, T., 2000. Anal. Sci. 16, 1013–1021.
Kariuki, J.K., McDermott, M.T., 2001. Langmuir 17, 5947–5951.
Katz, E., Filanovsky, B., Willner, I., 1999a. New J. Chem. 23, 481–487.
Katz, E., Lioubashevski, O., Willner, I., 2005. J. Am. Chem. Soc. 127, 3979–3988.
Katz, E., Shipway, A., Willner, I., 2003. Handbook of Fuel Cells—Fundamentals, Technology and Applications. John Wiley & Sons Ltd (Chapter 21—biochemical fuel cells).
Katz, E., Willner, I., Kotlyar, A.B., 1999b. J. Electroanal. Chem. 479, 64–68.
Kavanagh, P., Boland, S., Jenkins, P., Leech, D., 2009. Fuel Cells 9, 79–84.
Khani, Z., Jolivalt, C., Cretin, M., Tingry, S., Innocent, C., 2006. Biotechnol. Lett. 28, 1779–1786.
Kim, B.H., Chang, I.S., Gadd, G.M., 2007. Appl. Microbiol. Biotechnol. 76, 485–494.
Kim, H.H., Mano, N., Zhang, Y., Heller, A., 2003. J. Electrochem. Soc. 150, 209–213.
Kim, J., Grate, J., Wang, P., 2008. Trends Biotechnol. 26, 639–646.
Kim, J., Jia, H., Wang, P., 2006. Biotechnol. Adv. 24, 296–308.
Kim, J., Kim, S.I., Hwa Yoo, K., 2009. Biosens. Bioelectron. 25, 335–350.
Kjeang, E., Sinton, D., Harrington, D., 2006. J. Power Sources 158, 1–12.
Kontani, R., Tsujimura, S., Kano, K., 2009. Bioelectrochemistry 76, 10–13.
Kuwahara, T., Homma, T., Kondo, M., Shimomura, M., 2009. Syn. Met. 159, 1859–1864.
Larminie, J., Dicks, A., 2003. Fuel Cell Systems Explained. John Wiley & Sons.
Lee, J.Y., Shin, H.Y., Kang, S.W., Park, C., Kim, S.W., 2010. J. Power Sources 195, 750–755.
Lee, J.Y., Shin, H.Y., Lee, J.H., Song, Y.S., Kang, S., Park, C., Kim, J.B., Kim, S.W., 2009. J. Molec. Catal. B 59, 274–278.
Lehr, J., Williamson, B.E., Barrière, F., Downward, A.J., 2010. Bioelectrochemistry 79, 142–146.
Lim, J., Malati, P., Bonet, F., Dunn, B., 2007. J. Electrochem. Soc. 154, A140–A145.
Lin, J., Brown, C.W., 1997. Trends Anal. Chem. 16, 200–211.
Lin, Y., Lu, F., Tu, Y., Ren, Z., 2004. Nano Lett. 4, 191–195.
Liu, H., Cheng, S., Logan, B.E., 2005a. Environ. Sci. Technol. 39, 5488–5493.
Liu, H., Grot, S., Logan, B.E., 2005b. Environ. Sci. Technol. 39, 4317–4320.
Liu, H., Logan, B.E., 2004. Environ. Sci. Technol. 38, 4040–4046.
Lovley, D.R., 2006. Curr. Opin. Biotechnol. 17, 327–332.
Mano, N., 2008. Chem. Commun. 19, 2221–2223.
Mano, N., Fernandez, J.L., Kim, Y., Shin, W., Bard, A.J., Heller, A., 2003. J. Am. Chem. Soc. 125, 15290–15291.
Mano, N., Kim, H.H., Zhang, Y.C., Heller, A., 2002a. J. Am. Chem. Soc. 124, 6480–6486.
Mano, N., Mao, F., Heller, A., 2002b. J. Am. Chem. Soc. 124, 12962–12963.
Mano, N., Mao, F., Heller, A., 2005. J. Electroanal. Chem. 574, 347–357.
Mao, F., Mano, N., Heller, A., 2003. J. Am. Chem. Soc. 125, 4951–4957.
Marcus, A.K., Torres, C.I., Rittmann, E., 2007. Biotechnol. Bioeng. 98, 1171–1182.
Miyake, T., Oike, M., Yoshino, S., Yatagawa, Y., Haneda, K., Kaji, H., Nishizawa, M., 2009. Chem. Phys. Lett. 480, 123–126.
Moehlenbrock, M.J., Minteer, S.D., 2008. Chem. Soc. Rev. 37, 1188–1196.
Niessen, J., Schröder, U., Harnisch, F., Scholz, F., 2005. Lett. Appl. Microbiol. 41, 286–290.
Osman, H., Shah, A.A., Walsh, F.C., 2010. Biosens. Bioelectron. 26, 953–963.
Park, D.H., Zeikus, J.G., 2003. Biotechnol. Bioeng. 81, 348–355.
Patolsky, F., Weizmann, Y., Willner, I., 2004. Ang. Chem. 43, 2113–2117.

Pellissier, M., Barrière, F., Downward, A.J., Leech, D., 2008. Electrochem. Commun. 10, 835–838.

Picioreanu, C., Head, I.M., Katuri, K.P., van-Loosdrecht, M.C.M., Scott, K., 2007. Water Res. 41, 2921–2940.

Picioreanu, C., van Loosdrecht, M.C.M., Curtis, T.P., Scott, K., 2010. Bioelectrochemistry 78, 8–24.

Pizzariello, A., Stredansky, M., Miertus, S., 2002. Bioelectrochemistry 56, 99–105.

Rabaey, K., Verstraete, W., 2005. Trends Biotechnol. 23, 291–298.

Ramanavicius, A., Kausaite, A., Ramanaviciene, A., 2008. Biosens. Bioelectron. 24, 761–766.

Ramanavicius, A., Kausaitea, A., Ramanaviciene, A., 2005. Biosens. Bioelectron. 20, 1962–1967.

Rosenbaum, M., Schroöder, U., Scholz, F., 2005. Environ. Sci. Technol. 39, 6328–6333.

Rozendal, R.A., Hamelers, H.V.M., Euverink, G.J.W., 2006. Int. J. Hydrogen Energy 31, 1632–1640.

Saby, C., Ortiz, B., Champagne, G.Y., Bélanger, D., 1997. Langmuir 13, 6805–6813.

Sakai, H., Nakagawa, T., Tokita, Y., Hatazawa, T., Ikeda, T., Tsujimura, S., Kano, K., 2009. Energy Environ. Sci. 2, 133–138.

Sarma, A.K., Vatsyayan, P., Goswami, P., Minteer, S.D., 2009. Biosens. Bioelectron. 24, 2313–2322.

Schoenfisch, M.H., Pemberton, J.E., 1998. J. Am. Chem. Soc. 120, 4502–4513.

Shah, A.A., Ralph, T.R., Walsh, F.C., 2009. J. Electrochem. Soc. 156, B465–B484.

Shah, A.A., Walsh, F.C., 2008. J. Power Sources 185, 287–301.

Shah, A.A., Watt-Smith, M., Walsh, F., 2008. Electrochim. Acta 53, 8087–8100.

Sheldon, R.A., 2007. Adv. Synth. Catal. 349, 1289–1307.

Shukla, A.K., Suresh, P., Berchmans, S., Rajendran, A., 2004. Curr. Sci. 87, 455–468.

Solomon, E.I., Sundaram, U.M., Machonkin, T.E., 1996. Chem. Rev. 96, 2563–2606.

Soukharev, V., Mano, N., Heller, A., 2004. J. Am. Chem. Soc. 126, 8368–8369.

Stoica, L., Dimcheva, N., Ackermann, Y., Karnicka, K., Guschin, D.A., Kulesza, P.J., Rogalski, J., Haltrich, D., Ludwig, R., Gorton, L., Schuhmann, W., 2009. Fuel Cells 9, 53–62.

Sucheta, A., Cammack, R., Weiner, J., Armstrong, F.A., 1993. Biochemistry 32, 5455–5465.

Tamaki, T., Ito, T., Yamaguchi, T., 2007. J. Phys. Chem. B 111, 10312–10319.

Tamaki, T., Yamaguchi, T., 2006. Ind. Eng. Chem. Res. 45, 3050–3058.

Tasca, F., Gorton, L., Harreither, W., Haltrich, D., Ludwig, R., Nöll, G., 2008a. J. Phys. Chem. C 112, 9956–9961.

Tasca, F., Gorton, L., Harreither, W., Haltrich, D., Ludwig, R., Nöll, G., 2008b. J. Phys. Chem. C 112, 13668–13673.

Tischer, W., Wedekind, F., 2000. In: Wolf-Dieter, F., (Ed.), Biocatalysis—From Discovery To, Applications, Springer-Verlag. 95–126.

Togo, M., Takamura, A., Asai, T., Kaji, H., Nishizawa, M., 2007. Electrochim. Acta 52, 4669–4674.

Togo, M., Takamura, A., Asai, T., Kaji, H., Nishizawa, M., 2008. J. Power Sources 178, 53–58.

Topcagic, S., Minteer, S.D., 2006. Electrochim. Acta 51, 2168–2172.

Treu, B.L., Minteer, S.D., 2008. Bioelectrochem. 74, 73–77.

Tsujimura, S., Kano, K., Ikeda, T., 2005. Electroanal. Chem. 576, 113–120.

Vincent, K.A., Cracknell, J.A., Lenz, O., Zebger, I., Friedrich, B., Armstrong, F.A., 2005. Proc. Natl. Acad. Sci. U. S. A. 102, 16951–16954.

Wang, D., Chen, L., 2009. Electrochim. Acta 54, 4316–4320.

Wang, J., 1999. Anal. Chim. Acta 399, 21–27.

Wang, J., Musameh, M., Lin, Y., 2003. J. Am. Chem. Soc. 125, 2408–2409.

Wang, S.C., Yang, F., Silva, M., Zarow, A., 2009. Electrochem. Commun. 11, 34–37.

Watanabe, K., 2008. J. Biosci. Bioeng. 106, 528–536.

Willner, I., Arad, G., Katz, E., 1998a. Bioelectrochem. Bioener. 44, 209–214.

Willner, I., Heleg-Shabtai, V., Blonder, R., Katz, E., Tao, G., 1996. J. Am. Chem. Soc. 118, 10321–10322.

Willner, I., Katz, E., Patolsky, F., Bückmann, A.F., 1998b. J. Chem. Soc., Perkin Trans. 2, 1817–1822.

Willner, I., Yan, Y.M., Willner, B., Tel-Vered, R., 2009. Fuel Cells 9, 7–24.

Xiao, Y., Patolsky, F., Katz, E., Hainfeld, J.F., Willner, I., 2003. Science 21, 1877–1881.

Yan, Y.M., Baravik, I., Tel-Vered, R., Willner, I., 2009. Adv. Mater. 21, 4275–4279.

Zayats, M., Katz, E., Willner, I., 2005. J. Am. Chem. Soc. 127, 12400–12406.

Zayats, M., Willner, B., Willner, I., 2008. Electroanalysis 20, 583–601.

Zebda, A., Renaud, L., Cretin, M., Innocent, C., Pichot, F., Ferrigno, R., Tingry, S., 2009a. J. Power Sources 193, 602–606.

Zebda, A., Renaud, L., Cretin, M., Pichot, F., Innocent, C., Ferrigno, R., Tingry, S., 2009b. Electrochem. Commun. 11, 592–595.

Zeng, Y., Choo, Y.F., Kim, H.H., Wu, P., 2010. J. Power Sources 195, 79–89.

Zhang, S.G.W.Q., Wang, R., Yoona, S.F., 2003. Biochem. Biophys. Res. Commun. 311, 572–576.

Zhao, X., Jia, H., Kim, J., Wang, P., 2009. Biotechnol. Bioeng. 104, 1068–1074.

Zheng, W., Zhou, H.M., Zheng, Y.F., Wang, N., 2008. Chem. Phys. Lett. 457, 381–385.

Zhou, M., Deng, L., Wen, D., Shang, L., Jin, L., Dong, S., 2009. Biosens. Bioelectron. 24, 2904–2908.